Defining the limits to long-term nano-indentation creep measurement of viscoelastic materials

Hou, X. & Jennett, N. M.

DOI 10.1016/j.polymertesting.2018.07.022
ISSN 0142-9418
ESSN 1873-2348
Publisher: Elsevier

Defining the limits to long-term nano-indentation creep measurement of viscoelastic materials

X.D. Hou[a,b] and N.M. Jennett[a]

[a] Coventry University, Priory Street, Coventry, West Midlands, CV1 5FB, UK
[b] National Physical Laboratory, Teddington, Middlesex, TW110LW, UK
Corresponding author: Xiaodong Hou (email: xiaodong.hou@coventry.ac.uk)

Abstract

An ultra-stable instrumented nano-indentation tester (UNHT, Anton Paar) was used to study extremely long (30000 seconds) indentation creep of polymers. Total drift rate, measured on fused silica and sapphire samples, was less than 0.2 pm/second for up to 10 hours, enabling collection of valid, low-uncertainty, long-term creep data - orders of magnitude longer than previously possible. Fits of the popular *N*-element Kelvin model to indentation creep data gave values of instant elastic modulus E_0^* and infinite modulus E_∞^* strongly dependent on the time-span of data fitted. Comparison with the long-term experimental data showed that the model was unable to use short term data to predict creep at the much longer times required by industry. A new analysis method is proposed to obtain a better estimate of the true value of infinite modulus, E_∞^*, which is the simplest indicator of maximum dimensional change of polymeric material components subject to long-term stress.

Key words: indentation, long-term creep, viscoelastic, modulus

1. Introduction

Polymeric material components are increasingly used in many industries, such as automotive and aerospace, as lightweight replacements for metal parts, to improve overall energy efficiency and reduce carbon emissions [1,2,3]. Accurate dimensional control and stability is crucial for the success of a polymeric product, especially when a component is subject to a constant load over an extended period of time. Compared to metal or ceramic components, polymers exhibit more pronounced time dependent properties and deform continuously (creep) under an externally applied load. Creep is often the life limiting property of polymer components. Their creep behaviour is, therefore, of great interest to allow accurate prediction of component life time. The simplest test setup to measure uniaxial creep uses dead weights to provide a constant applied force (stress) and measures the creep (displacement) using an extension-measuring device; this kind of setup can be used to test long-term creep (months to years) with very little effort. Controlled force uniaxial mechanical testing instruments are also frequently used for polymer creep measurements, which allow more control of the running experiments (i.e. easy change of applied load during the creep). These creep measurement methods are well established and even standardized [4].

In recently years, the increasing demand for miniature, pocket-sized and compact devices, is requiring material components (including polymeric components) to be made smaller. The reduced dimensions are a challenge for traditional mechanical testing techniques, as the specimen isn't big enough to meet standard measurement requirements, and can't be made large and stay representative of the original component. To address this issue, instrumented Indentation testing (IIT) is becoming popular as a useful tool, capable of testing small volumes of materials [5,6]. IIT-based creep testing can provide high-resolution mechanical property mapping as the contact size can be reduced down to the sub-micrometre range, commonly called nano-indentation. This technique is particularly useful for probing the mechanical properties of individual phases in composite materials such as fibre reinforced polymeric matrix composites used in the aeronautical industry, where, nano-indentation is the only technique that can be used to get the properties of the matrix (i.e. resin pockets) of the final composite.

As in macro-scale rheology, indentation creep measurements measure longer time constant effects (properties) than oscillation methods such as Dynamic Mechanical Analysis (DMA), which produces distinctly different (frequency dependent) results. Rapid AC oscillation dynamic indentation methods also exist but typically require additional hardware, whereas, indentation creep measurements can be made by any instrumented indentation system capable of force control (without any additional equipment). All that is required is a ramp in force followed by holding the indenter at the selected test force for a period of time to monitor the creep compliance, i.e. the indentation displacement vs. time as the indenter creeps into the sample [7,8]. The measurement stability of the instrument and the thermal (or other drift) sensitivity of the instrument to its unique environment determine the uncertainty of the creep and creep rates measured. This sets the minimum creep rate that can be measured acceptably/validly. Thermal expansion induced displacement is a particular problem. The measured indentation displacement includes all components of displacement (including thermal drift) within the "measurement loop". Thermal expansion can be considerable and, as most IIT systems are "bottom referenced" (the entire frame of the machine is included in the displacement measurement loop), a considerable amount of thermally induced displacement drift can be included in the test results. Tests in the EC INDICOAT project showed that systems with a thermal expansion of 1000 nm/K are not unusual [9]. In quasi-static IIT tests on non-viscous materials, the thermal drift can be measured and subtracted by measuring the indentation displacement of a stable contact at constant force over a period of time; typically a constant average drift rate is assumed and a linear correction is applied to the displacement data [10]. Since stable contacts are not possible for any material that creeps, indentation creep data cannot be corrected using this method.

An alternative method when performing dynamic IIT tests on non-viscous materials, is to use the reference modulus method to estimate the drift rate by calculating the area of contact (and thence actual contact depth) from the values of contact stiffness continuously measured during the indentation cycle[11]. This method assumes the elastic modulus of the sample remains constant with both indent size and indent depth, and also with time. The method requires the IIT system to have the necessary oscillation hardware and presumes that there is no change in properties of the contact as a function of shear rate or hysteretic adiabatic heating of the material as a function of frequency. In an investigation where the aim is to measure the (potentially variable) elastic modulus of a material using instruments not equipped for dynamic indentation, assuming these things is not appropriate, so thermal drift cannot be calculated using this method either. Indentation instrument drift is an increasingly significant contribution to the total creep data as the contact size decreases. This is particularly the case for long-term indentation creep measurements, where the creep rate is reducing over time, but the thermal drift is constant and accumulates over time. As a result, indentation creep tests, especially nano-indentation creep tests, are normally of short duration (e.g. tens of seconds) to minimise this problem. It is clear that much longer nano-indentation creep measurements on viscoelastic materials are desirable if long term creep is the lifetime determining property of a material or component. This is a challenge that requires a stable IIT measurement system with extremely low thermal drift to overcome.

Standard rheological material mechanical ('kinematic') models can be used to model and simulate indentation creep in order to assign fixed property parameter values to describe the viscous behaviour of polymeric materials [8,12]. The models adopted here used linear-elastic "Hookean springs" and "Newtonian dashpots" to represent the combination of the instant response (the purely elastic component) and a time-dependant material response (the viscous component) [13, 14, 15]. Normalising to the area of contact converts these spring constants and damping coefficients to values of modulus and viscosity that can be used as representative parameters to describe the material viscoelastic properties. It is commonly assumed that any plastic deformation is negligible for shallow indentations [16]. In principle, the mathematical response functions of these models can be fitted to indentation data and the indentation-derived parameter values for modulus, viscosity and time

constant for the material and this function used to calculate the longer term creep of the material. (Expectations derived from uniaxial rheology might expect up to two decades time longer than the experimental duration). This would be very useful to accelerate the prediction of creep behaviour of polymeric components expected to serve a long-life time. However, the reality is that there is little evidence for the validation of such models, due to the lack of high quality long-term nano-indentation creep data.

In this study, an IIT platform with extremely low thermal drift (< 0.2 pm/second) was used to obtain extremely long indentation creep data (30,000 seconds) from a piece of commercial polymer (PS-3). The long duration indentation creep data was then used to investigate the appropriate number of elements required for creep simulation using a generalized *n*-time-constant (*N* = 2*n*+1 elements) Kelvin viscoelastic model. A new method is also proposed to obtain a more robust estimate of the indentation time-independent modulus (E_{∞}^{*}).

2. Viscoelastic model for creep data analysis

The linear elastic contact with a conical-pyramidal indenter is normally given by [17,18]:

Equation 1 $$\boldsymbol{P = \frac{A}{2}\, E^{*}\, cot\varphi}$$

where *P* is the contact force, *A* is the contact area, *E** is the indentation elastic modulus and $\boldsymbol{\varphi}$ is the cone semi-angle.

The expression in Equation 1 can be rewritten to include linear viscoelasticity by replacing the elastic constant *P*/*E** with integrals involving the creep response functions *J*(*t*) [19]:

Equation 2 $$\boldsymbol{A(t) = 2\int_0^t J(t-u)\frac{dP(u)}{du}du}$$

where *A*(*t*) is the contact area with time and u is a dummy variable for integration that takes into account the incrementing of the applied force over a finite time.

In this study, the maximum indentation displacement was about 2 µm, which is below the 6 µm limit specified in ISO 14577 for the use of a perfect indenter geometry (with less than a 1% error in contact area due to tip rounding effects) [10]. The actual area function of the Berkovich nano-indenter used in this study was, therefore, obtained directly by a metrological atomic force microscope (AFM). Indentation displacement, *h*, can be relatively large when investigating soft materials, and in other studies, where close to mm penetration depths were reported, an assumption of perfect (ideal shape) indenter geometry was used [20, 21]. This simplification enables the contact area in Equation 2 to be easily expressed as a function of the indentation displacement. For bigger indenters and indentation depths, optical methods can be a more convenient way for three-dimensional shape measurement, even for high slope angles [22].

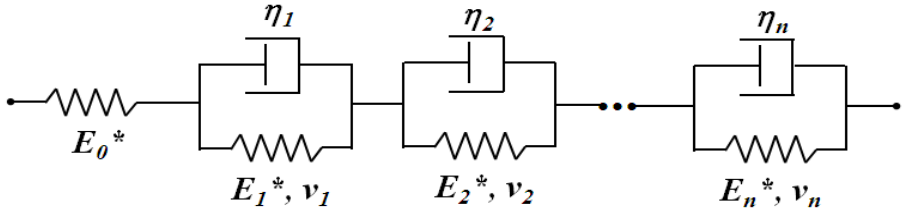

Figure 1 The generalised *N* (= 2*n* + 1)-element Kelvin model to simulate the viscoelastic behaviour; when *N* = 2n+1 =3, it is known as the standard linear solid (SLS) model.

The generalised *n*-time-constant (*N = 2n + 1* elements) Kelvin model was used to simulate the viscoelastic behaviour, as shown in Figure 1. The creep function corresponding to the *N*-element Kelvin model is:

Equation 3 $$\boldsymbol{J(t) = \frac{1}{E_0^*} + \sum_{i=1}^{n}\left\{\frac{1}{E_i^*}\left[1 - exp\left(\frac{-t}{\tau_i}\right)\right]\right\}}$$

where the creep compliance *J*(*t*) is the sum of the instantaneous elastic response ($1/E_0^*$) and a response from a series of n pairs of parallel springs and dashpots. Creep compliance is zero at *t*=0 and increases to $\sum \frac{1}{E_i^*}$ after an infinite time, E_0^* is the instantaneous storage indentation modulus, τ_i are the time constants and E_i^* is the corresponding modulus for each of the time constant (1 to *n*).

A full derivation of the indentation contact area vs. time response for a standard linear solid (SLS) model (*n* = 1 time constant) has been published previously [14]. This calculates the total indentation creep, including the creep that occurs during the linear loading segment assuming it takes a time t_0 to reach the required indentation force P_0. This expression is expanded in this study to the *N*-element Kevin model as given below:

Equation 4 $$\boldsymbol{A = 2\left\{\left(\frac{t_0}{E_0^*} + \sum\frac{t_0}{E_i^*}\right) - \sum_{i=1}^{n}\left[\left(\frac{\tau_i}{E_i^*}\right)exp\left(\frac{-t}{\tau_i}\right)\left(exp\frac{t_0}{\tau_i} - 1\right)\right]\right\}}$$

The expression used to fit the creep data (*A* vs. *t*) is:

Equation 5 $$\boldsymbol{A(t) = C_0 + \sum_{i=1}^{n} C_i exp\left(\frac{-t}{\tau_i}\right)}$$

Where C_0, C_i and τ_i are fitting parameters obtained by curve fitting; from which the instant modulus at time zero (E_0^*) and the moduli at any particular time constant (E_i^*) may be found by comparing Equation 4 and Equation 5:

Equation 6 $$\boldsymbol{E_0^* = \left(\frac{1}{2}\cdot C_0 - \sum_{i=1}^{n}\frac{1}{E_i^*}\right)^{-1}}$$

Equation 7 $$\boldsymbol{E_i^* = -2\cdot\frac{\tau_i}{C_i}\cdot\left(exp\frac{t_0}{\tau_i} - 1\right)}$$

The modulus for an infinite time response ($\boldsymbol{E_\infty^*}$) for any give *N*-element model can then be obtained:

Equation 8: $$\boldsymbol{E_\infty^* = \left(\frac{1}{E_0^*} + \sum_{i=1}^{n}\frac{1}{E_i^*}\right)^{-1} = \left(C_0\cdot\frac{A}{2}\right)^{-1}}$$

The indentation moduli (E_0^* and E_∞^*) are plain strain moduli; they can be converted to comparable *Y*oung's moduli using the relationship:

Equation 9: $$\boldsymbol{\frac{1}{E^*} = \frac{(1-\nu^2)}{E}}$$

where *E**, *E* and *v* describe plain strain modulus, Young's modulus and Poisson's ratio respectively.

3. Experimental details

To reduce instrument drift to a minimum, an Ultra Nanoindentation Tester (UNHT, CSM Instruments SA now Anton Paar) was used in this study. The UNHT measurement head is constructed of ZeroDur® ceramic to reduce dimensional sensitivity to temperature change. The indentation system was located in a laboratory environment with temperature variation less than 0.1 K (Nano-mechanics Lab, National Physical Laboratory, Teddington, UK). The UNHT features a unique dual indenter design. One indenter

is used for indentation whilst the other one provides active surface referencing, to minimise thermal drift and frame compliance in real experimental time [23]. This cuts out all but the measurement head from the measurement loop. With both the reference and the indenter on the sample surface, the thermal drift experienced is essentially limited to the differential thermal expansion between the reference and the indentation indenter shafts (the rest of the head being made of ZeroDur®). Expansion of the rest of the instrument frame and the sample itself is nulled out by the surface reference.

To measure the stability of the UNHT, two samples were used: fused silica and sapphire. These two materials have well-known mechanical properties and are widely used for the calibration of instrumented indentation systems, including the indenter area function and instrument frame compliance. The indenter was brought into contact, the force increased, and then held at a constant value for 10 hours (36000 seconds), whilst the indentation displacement data vs. time was measured and recorded. The temperature variation inside the UNHT chamber was measured and found to vary by only ±0.01°C during the experimental cycles; the noise floor of the indentation force was observed to be less than 2 μN.

The commercially available material denoted PS-3 (Vishay Micro-Measurements, Raleigh, NC, USA) was selected as a candidate polymer to study the long-term indentation creep behaviour. This material is expected to be viscoelastic and it is highly homogeneous with good surface finish. The elastic modulus of PS-3 declared by the vendor is 0.21 GPa, but no information was provided regarding the time scale or method used for obtaining such a value [24]. Indentation creep experiments were performed consisting of a constant-rate force-increase ramp (duration 3 seconds) followed by a 30000 seconds hold at a constant test force. The UNHT design uses direct measurement of the indentation force and does not have to correct for a suspension spring stiffness. This enables the indentation force to be kept constant even when there is significant creep displacement. The experimental details are summarized in Table 1.

Table 1 Summary of the nano-indentation creep experiments in this study

Material	Indenter shape	Maximum test force	Creep time	Experimental details
Fused silica	Berkovich	1 mN	36000 seconds (10 hours)	No thermal drift hold periods used.
Sapphire	Berkovich	9 mN	36000 seconds (10 hours)	An additional 1hour “thermal drift” hold was inserted after contact at 90% force removal.
PS-3	Berkovich	1 mN	30000 seconds	Loading/unloading time: 3 seconds

4. Results

4.1 The stability of the instrumented nano-indentation tester UNHT

Figure 2 and Figure 3 clearly show that the measured indentation displacement at the beginning of the holding period increases with time for both the fused silica and sapphire specimens. Over time, the creep rate significantly reduces; the last hour of the hold exhibits extremely low additional creep (< 1nm). It can be seen that the creep rate (averaged over 1 hour) for fused silica decays to approximately zero, whilst the creep rate in the sapphire appears to asymptote to a constant positive value of ~ 0.1 pm/second. If the total displacement after reaching maximum test force is assumed to be drift and is averaged over the full hold period of 10 h, then the averaged drift rate in the 1 mN

fused silica experiment was 1.8 nm/hour (0.5 pm/second) and that in the 9 mN sapphire experiment 0.6 nm/hour (0.17 pm/second).

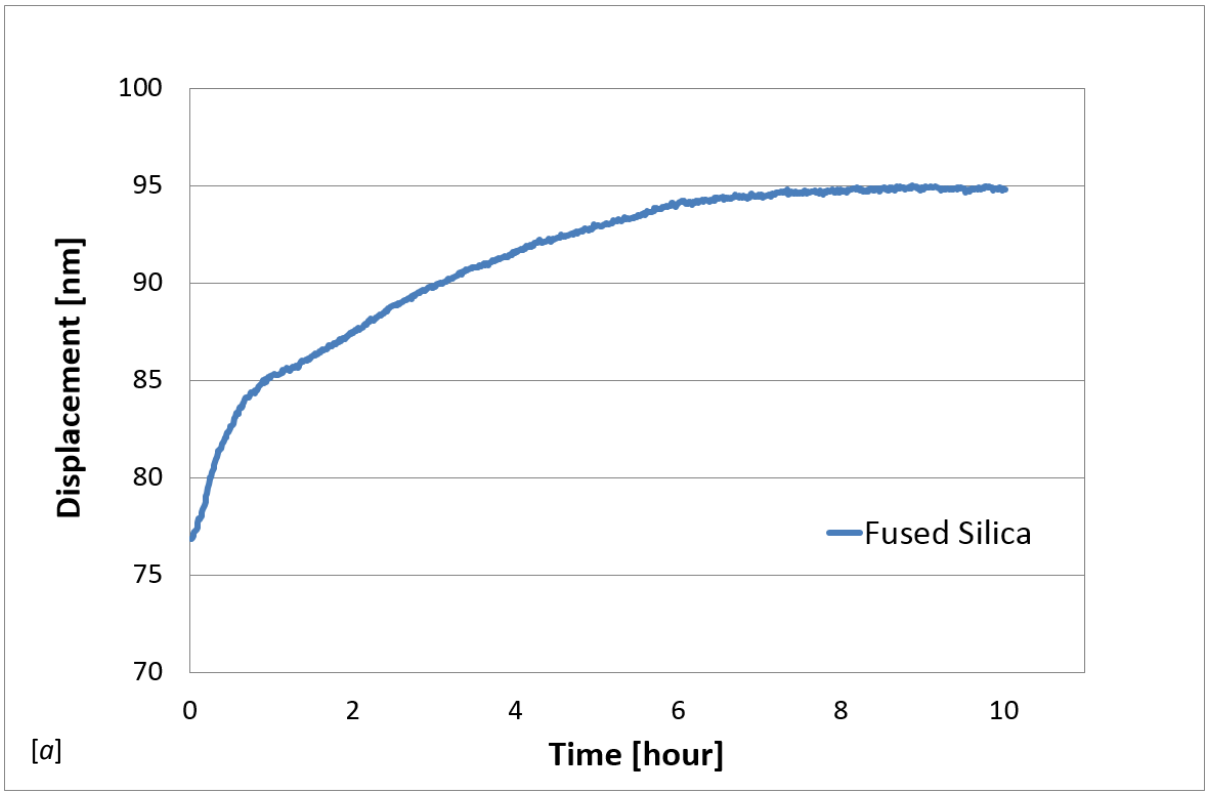

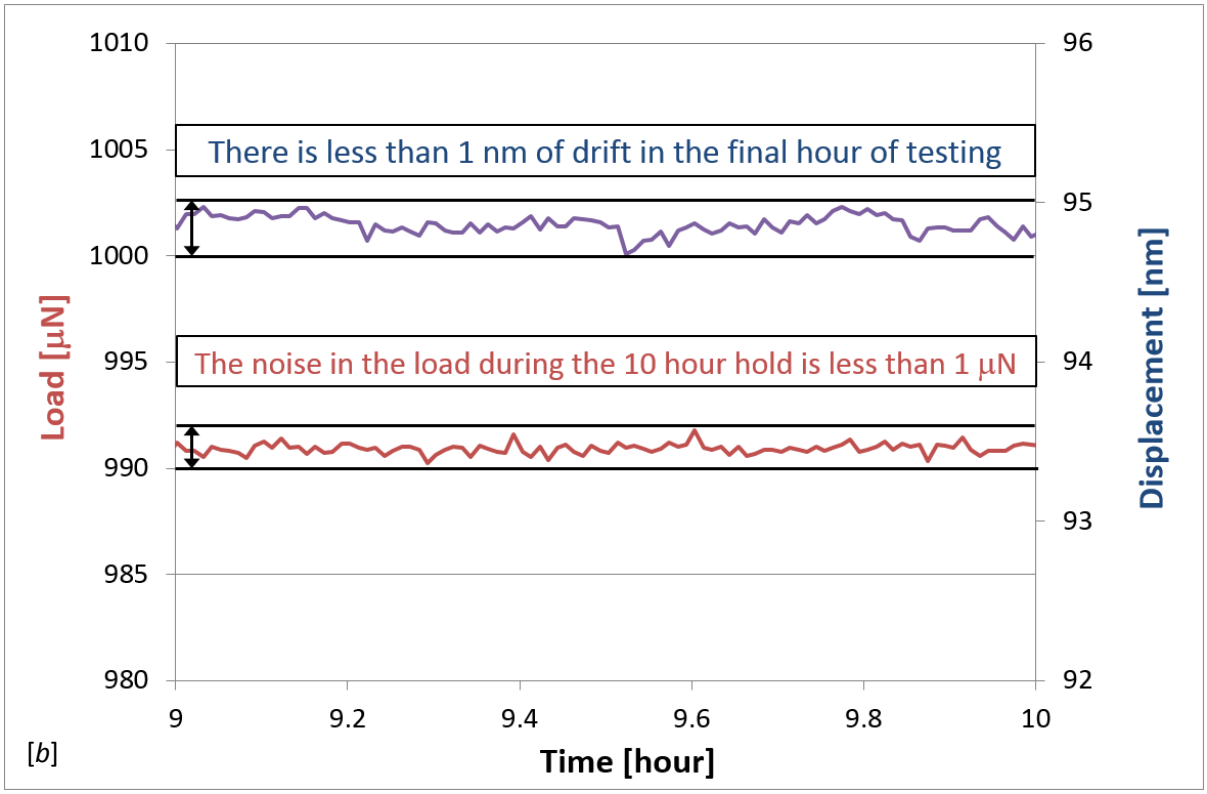

Figure 2 [*a*] The 10 hour indentation creep on fused silica using a Berkovich indenter, the averaged drift rate is estimated to be 0.5 pm/second; [*b*] the measured indentation load and displacement data in the last hour of creep exhibits extremely stable contact (< 1 μN) and low additional creep (< 1 nm).

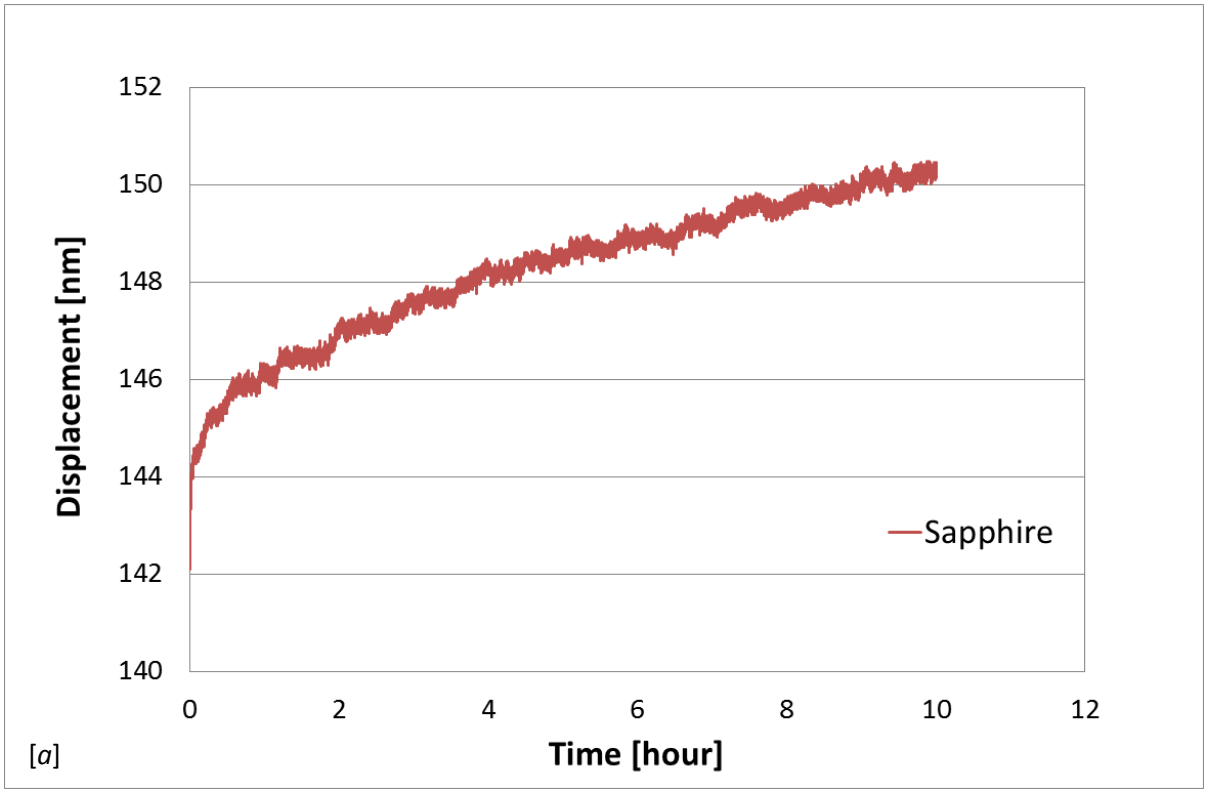

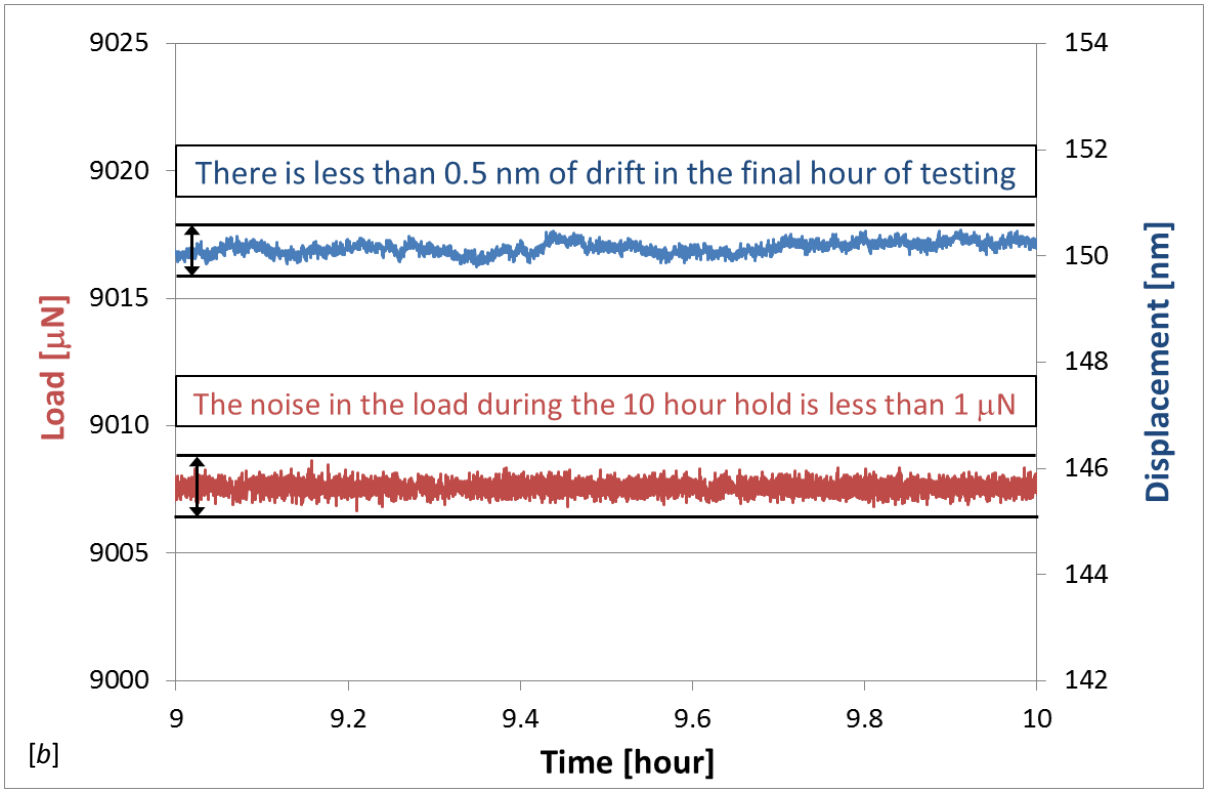

Figure 3 [*a*] The 10 hour indentation creep on sapphire using a Berkovich indenter, the averaged drift rate is estimated to be 0.17 pm/second; [*b*] the measured indentation load and displacement data in the last hour of creep exhibits extremely stable contact (< 1 μN) and low additional creep (< 0.5 nm).

4.2 Indentation creep of PS-3

Indentation creep data was collected at a data acquisition rate of 10 Hz. Considering the longest creep time for this study is 30000 seconds, the indentation creep raw data files generated were very large, hence difficult to handle using standard desktop computing power. The fixed acquisition rate generated data points that were linearly spaced in time, whereas the viscoelastic model used to fit the data was linear in log time. To reduce the computing effort required and to avoid the results being heavily weighted towards longer time constants, the data density was reduced to only 100 data points per decade of creep time and evenly spaced in log time.

One issue arising from the use of a surface reference contact is that the reference contact itself may creep when in contact with viscous or creeping materials. In this study, we avoided this problem by placing the reference contact onto a reproducible, hard (sapphire) surface on the sample holder. The use of this "hard shoulder" allowed: reproducible contact conditions for the reference contact, the use of the same reference contact force for any sample, and avoided additional uncertainty due to surface roughness. The only downside was that it included a small additional differential thermal expansion component into the measurement loop, which slightly increased the thermal drift sensitivity of the instrument. Everything else in the sample stage being equal, the additional drift is the difference in thermal expansion between the sample and the same thickness of material in the hard shoulder (typically Al topped by 400 µm of sapphire). Assuming a difference in coefficient of thermal expansion (CTE) between sample and the hard shoulder of 10^{-4}/K, a sample thickness of 3 mm, and a temperature change of 1 mK/hour, this results in an additional drift rate of 0.08 pm/second; for a total temperature change of 10 mK, this results in a thermal expansion of approximately 3 nm. Given the expected creep rates of a sample, this is not significant. However, for a thicker sample in a less stable temperature environment, this might become significant, in which case, creating a step and setting a sapphire wafer into the surface of the sample would be an improvement.

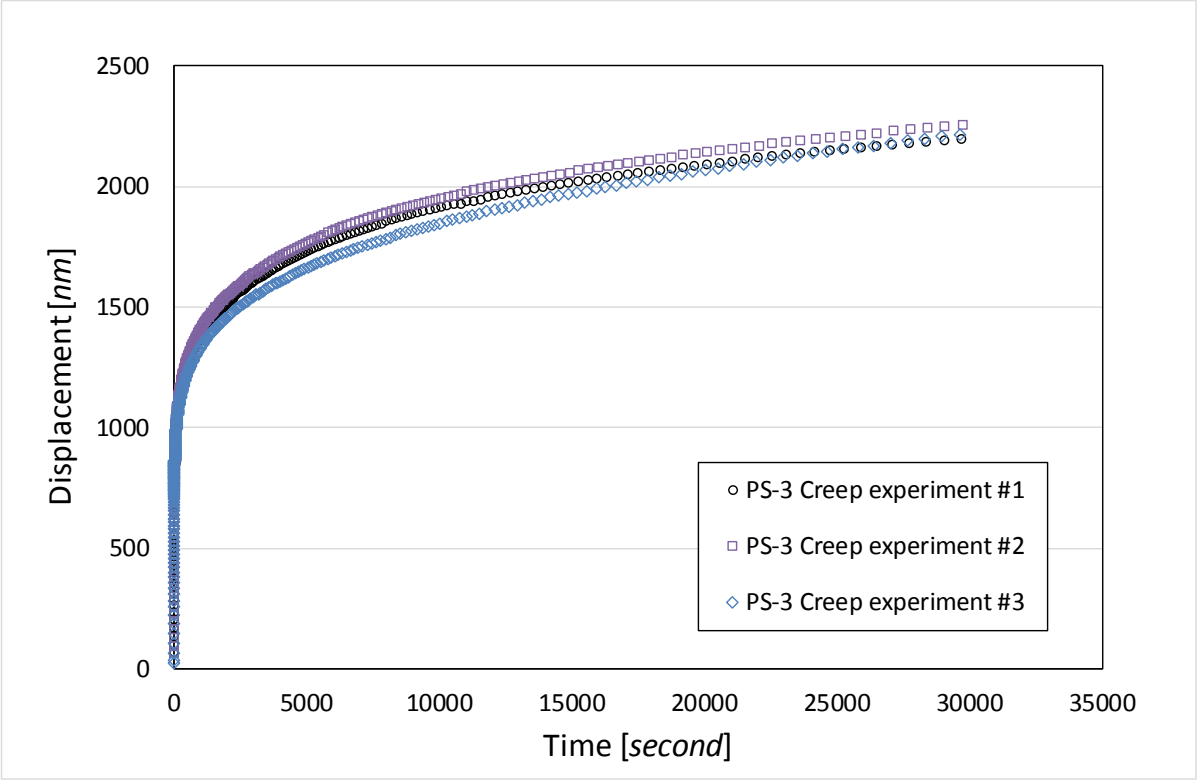

Figure 4 Three replicate indentation creep datasets obtained from PS-3 using a Berkovich indenter, each with durations of 30000 seconds at a constant 1 mN test force.

Three replicate indentation creep datasets each with a duration of 30000 seconds at a constant 1 mN test force were obtained from PS-3 and are plotted in Figure 4. The terminal creep rate at 30000 second in all cases was greater than 10 pm/second. This is at least 50 times the underlying combined drift and creep rate of the UNHT system (0.2 pm/second) measured on non-viscous materials, and demonstrates that the UNHT is an adequately stable platform for creep measurements of this duration on this material. Furthermore, the relatively low drift rate means that drift may be neglected and the creep curve assumed to consist only of the response of the PS-3 specimen under investigation. Significant variations in the creep data are, however, visible in figure 4. A difference in average creep rate and a variation in the instant total indentation depth achieved at the end of the increasing force ramp was observed. Given the stability of the instrument, this presumably comes from a variability in the sample indentation response in some way, possibly due to small material inhomogeneities causing spatial variation in both elastic and plastic properties. The use of a sharp-pointed, pyramidal indenter increases the possibility of instant plastic deformation, and will cause enhanced local creep at the beginning of the indentation cycle due to material experiencing the stress concentrations at the facet edges and at the tip. However, the volume of material affected is small in relation to the final indentation size, and the initially rapid creep rate soon exhausts itself via stress relaxation because the indentation rate is limited by the average stress of the indentation being much lower and decreasing as the proportion of edge to facet area decreases. [In brittle materials, such as fused silica and sapphire, cracking may occur at facet edges and the cracks may run over a period of time, generating additional initial indentation depth].

The *N*-element Kevin model described in section 2 was used to fit each creep curve with a series of models using different numbers of time constants. To investigate the effect of data length, the creep data was truncated at different creep times: 60, 1000, 6000 and 30000 seconds. The *N*-element Kelvin model with different numbers of elements (N = 3, 5, 7, 9, 11, 13 and 15) was then used to fit each truncated dataset and the fit results were compared. The data and the fits for the first 60 seconds of creep curve #3 are shown in Figure 5 for models with N = 3, 5, 7, and 15 elements. It can be seen that the popular standard linear solid (SLS) model (N = 3) doesn't fit the creep data well, especially at the beginning of the creep curve. By adding more elements, the fit was improved significantly and the maximum fitting residual was reduced from 15% (N = 3) to 1% (N = 7). Adding more elements (N > 7) to the model showed very little further improvement for this 60 seconds creep data set.

Fits to the longest indentation creep dataset (30000 seconds) from creep curve #3 are shown in Figure 6. It is clear that the SLS model is inadequate to fit the long creep data too - the fitting residuals are as high as 100%. Adding more elements into the model improved the fit significantly, but again, little further improvement was observed when more than 7 elements were used. From a mathematical point of view, increasing the number of elements increases the degrees of freedom to allow the fit to conform better to the creep curve shape. However, too many elements over-describes the problem and begins to fit the noise rather than the underlying functional form, resulting in fit parameter values that have little physical meaning.

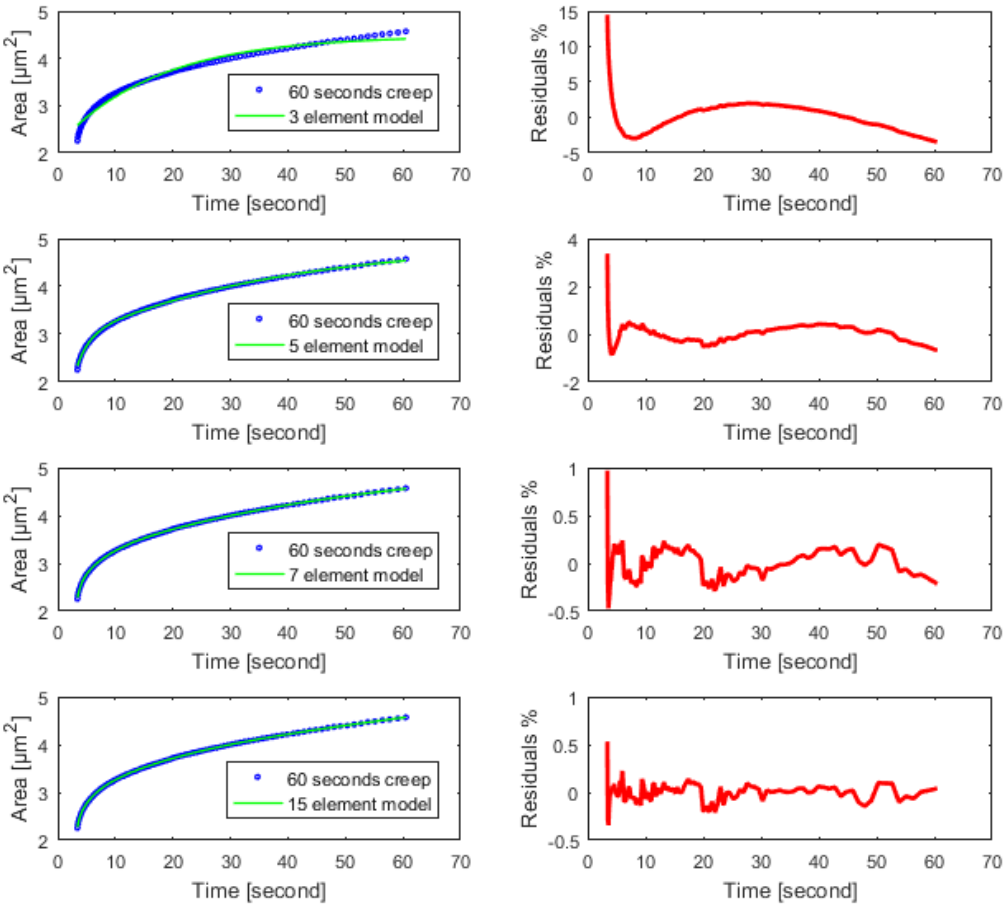

Figure 5 Left: The indentation creep (dataset #3) for the first 60 seconds obtained using a Berkovich indenter at 1 mN maximum test force. The fits were obtained using a generalized *N*-element Kelvin model when *N*=3, 5, 7 and 15. Right: the fitting residuals in percentage to show the goodness of the fit.

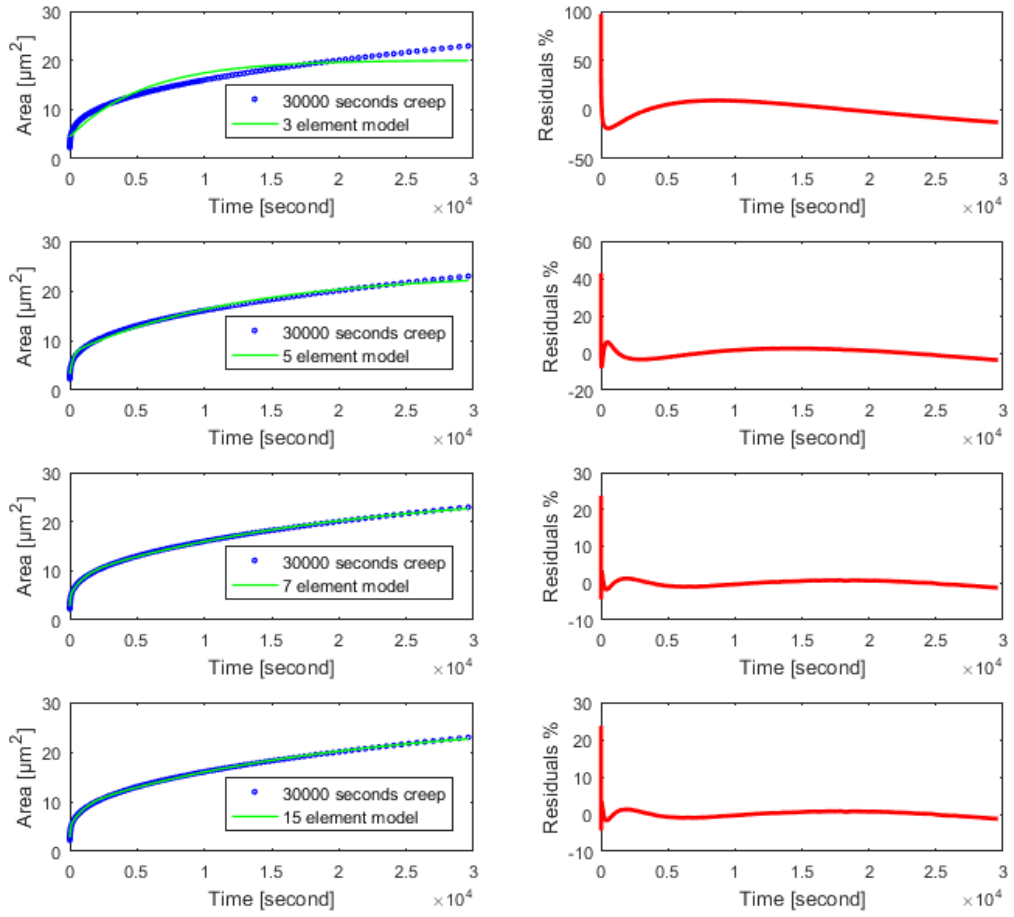

Figure 6 Left: The indentation creep (dataset #3) for the whole 30000 seconds obtained using a Berkovich indenter at 1 mN max test force. The fits were obtained using a generalized *N*-element Kelvin model when *N* =3, 5, 7 and 15. Right: the fitting residuals in percentage to show the goodness of the fit.

4.3 Viscoelastic analysis results

The values of instant modulus (E_0^*) obtained from fits to experimental creep curve #3 are plotted in Figure 7. Two trends are apparent: the calculated E_0^* increases when more elements are added to the *N*-element Kevin model; the E_0^* values obtained from the longer creep data are lower. Since E_0^* is the parameter quantifying the instant elastic response of a viscoelastic material under load, its value is very sensitive to the goodness of fit and the accuracy of the measurement data at the beginning of the creep hold. Adding more elements into the model improves the fit, generally by bending the fitting curve more toward the beginning of the creep hold and reducing the value of C_0 at low t values. This makes fit values of the corresponding contact area smaller and increases the calculated instant moduli (see Equation 6). This increase in E_0^* with increasing number of elements (from *N*=3 to *N*=7) is particularly strong for the results obtained from fitting the first 60 seconds creep. Fitting with more than 7 elements (*N*=9, 11, 13 and 15) makes little further improvement to the fit and the instant modulus was observed to plateau (except for one outlier point obtained from the 9-element fit). As a comparison, the fit to the full 30,000 s of creep data showed less variation in E_0^* upon adding more elements and also reached a plateau when more than 7-elements were used.

The values of instant modulus, E_0^*, for PS-3 obtained in this study fall within the range reported in the literature: Monclus et al reported E_0^* to be around 1.3 GPa, obtained by fitting a 3-element model to 60 seconds of indentation creep using a Berkovich indenter and assuming ideal (perfectly sharp) geometry [14]; but Oyen found E_0^* to be about 0.1 GPa when obtained by fitting a 5-element model to 120 seconds of indentation creep of a large radius spherical indenter (R = 150 µm) [25]. Assuming an indenter with perfect pyramidal shape without considering the tip rounding would tend to underestimate actual contact area and so overestimate modulus. Using a large radius spherical indenter will result in a more elastic (less plastically deformed) contact. These selected literature results were both obtained at 1 mN test force, and the difference between the two tip geometries will have caused the indentation penetration depths to have been very different (a factor of five).

The modulus values for infinite time response (E_∞^*) obtained from the different fits to experimental creep curve #3 are summarised in Figure 8. It can be seen that adding more elements and increasing creep time can both cause the calculated E_∞^* to decrease. Given that E_∞^* is the parameter that quantifies the accumulated viscoelastic deformation over an infinite creep time, this suggests that longer duration creep data will enable a more accurate prediction. The results show that longer creep time measurements yield a lower modulus value than predicted by exhaustion of the shorter time constant elements obtained from fitting or measuring shorter duration datasets. The results show that the SLS model is least capable of predicting the infinite time modulus and generates the largest error (a factor of two in this case). Similar to the E_0^* results, a big improvement was achieved by adding more elements into the model, increasing from 3 elements to 7 elements; but more than 7-element model provided little additional benefit. Experimental dataset #3 has been chosen as a representative case to reduce the number of plots, and additional viscoelastic analysis results are made available in the appendix.

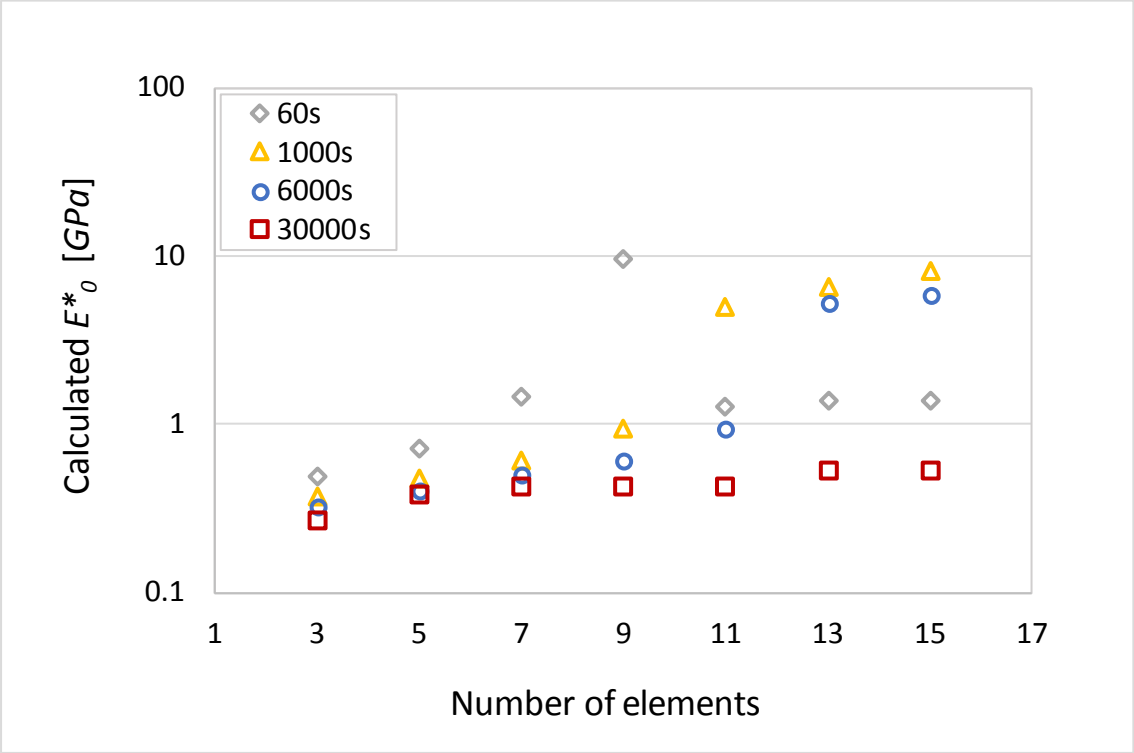

Figure 7 The instant modulus, E_0^*, obtained by fitting the 60, 1000, 6000 and 30000 seconds of the indentation creep curve (dataset #3) using a N-element Kelvin model (N = 3,5,7,9,11,13 and 15).

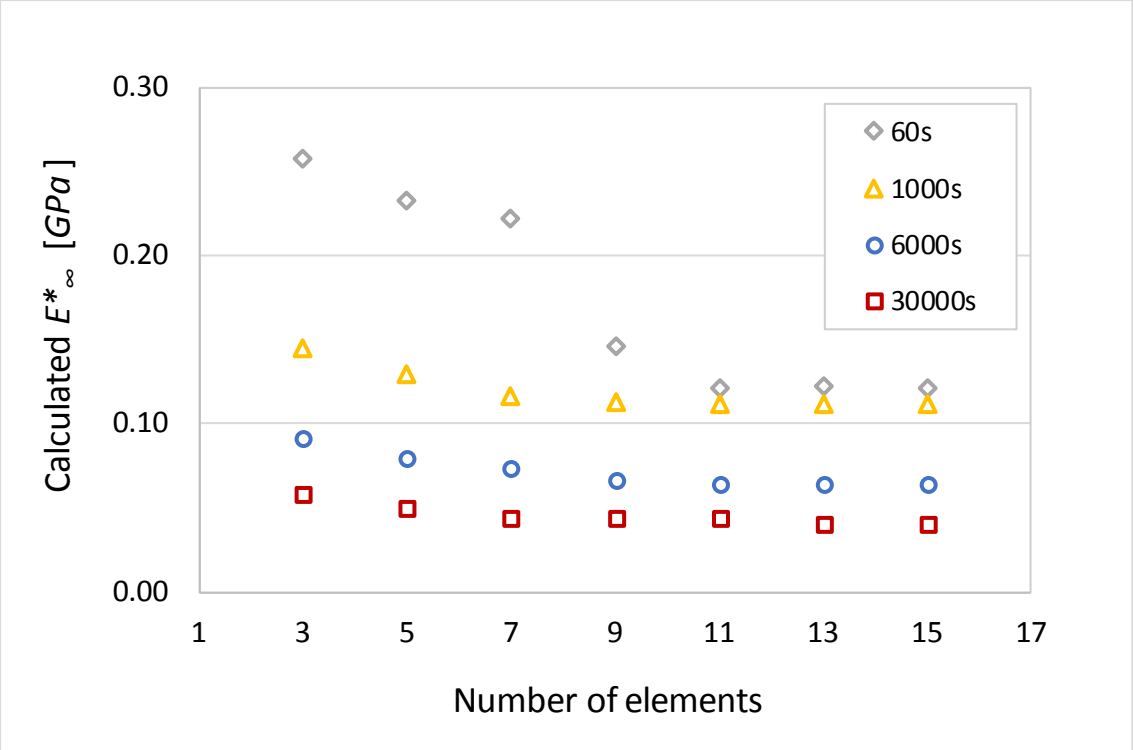

Figure 8 The effective infinite modulus, E^*_∞, obtained by fitting the 60, 1000, 6000 and 30000 seconds indentation creep curve (dataset #3) using a *N*-element Kelvin model (*N* = 3,5,7,9,11,13 and 15).

5 Discussion

5.1 Stability and drift as measured by contact with hard elastic surfaces

It is important to note that the measured indentation displacement drift is always a combination of the indenter creep into the material and the instrument drift (e.g. thermal drift). It is not possible to separate these two since an indentation test measures only the total displacement. Since thermal drift can be negative, it is possible for the measured creep displacement to be either reduced or increased by thermal drift. A non-viscous material is, therefore, required to characterise the drift rates in an IIT system. The ideal materials should exhibit little or no creep during a constant force hold period so that the displacement drift measured is independent of applied force and contact size. Any displacement should be due only to instrument (e.g. thermal) drift, which is typically seen as a constant drift rate. In practice it has been observed that a small, initially viscous, response is seen in most indentations, which has been attributed to squeezing out of surface capillary water layers or the settling of screw driven stages after recent movement [26]. As a consequence, ISO 14577 discards the initial part of a hold period when calculating the instrument drift rate using a constant force hold. Typically, the first 10 – 20 seconds of data is discarded [10]. Overall, the response expected from a non-creeping material is, therefore, a transient enhanced drift rate asymptoting to a constant drift rate. This is seen to be the sapphire response, which showed an initial ~144nm indentation followed by only 6 nm of creep at a rate varying very little over 10 hours. Fused silica, however, exhibited a much higher initial (and average) creep rate than sapphire and this creep rate decayed to be slightly negative. This suggests that the UNHT is easily capable of measuring the viscoelasticity of fused silica, and that the thermal drift rate in the fused silica experiment was possibly negative.

5.2 Viscoelastic analysis

Reliable E^*_0 values are surprisingly hard to obtain from this data. Despite the thermal drift rates being negligible, the fits to the data at the start of the creep hold periods are universally worse than the fit

at longer times. Even introducing many more fitting parameters fails to bring the residuals to the fit (Figure 5 and Figure 6) in line with those achieved at other time points in the same data set. This is despite having taken precautions to maintain constant data density with log time. This is a clear symptom of there being an error at the start of the dataset such as additional prompt plastic deformation in addition to the prompt elastic deformation (E_0^*). This problem has been raised before by Monclus [14] and Oyen [25]. One solution to this might be to include a plasticity displacement offset into the model, but this causes significant increase in the complexity of the integration. This was not attempted here as the ability to fit the longer time constant creep was not significantly affected, and so it was still possible to use the simpler equations presented here to investigate the ability to use shorter experiments to predict creep, creep rates and E_∞^* at longer times.

The change in the values of E_0^* and E_∞^* with the time span of creep data fitted is a significant problem for validation of the viscoelastic model and its application to indentation creep. If the model of visco-elasticity was correct, and if perfect, noiseless, infinite resolution data could be obtained, the fit should yield the same value for E_∞^* no matter what amount of data was collected or fitted. All time constants present in the material would be captured in the creep data and fitted exactly by the model. The material model proposed here effectively defines that the creep rate of the longer time constants is absolutely smaller than that of the shorter time constants (creep rates are assumed not to suddenly switch on or to accelerate with time). Thus, the longer the creep experiment, the lower the creep rate until all creep is exhausted at infinite time. In the real world of noise, there will be a resolution limit that is reached at some finite time, after which the small contribution of the very long time constants is not measurable. In uniaxial rheology it is generally accepted that the exponential model used effectively limits the sensitivity of measurement to one or two decades of time per time constant.

The very long duration creep datasets obtained in this study, (shown in Figure 9) vividly demonstrate deviation of the actual continued creep from the creep that can be mathematically predicted from fits to shorter data sets. In Figure 9[*a*], the experimental indentation curve for 30000 seconds (experiment #3) is superposed on simulated curves calculated using a viscoelastic 7-element model (parameters obtained by fitting the 10, 60, 1000, 6000 and 30000 seconds). It is clear that the simulated curves only continue to conform to the experimental curve shape in the region immediately beyond the fitting range, before they start to deviate rapidly ~~from the experimental curve~~. After only one decade of time beyond the fitted data range, the simulation curves have deviated completely from the experimental curve in both absolute value and functional form. It is clear that the prediction capability of the model is mathematically–quite limited: it can probably only be extrapolated to twice the experimental creep time, which is much less than the commonly accepted one or two decades of time. The corresponding E_∞^* values calculated using these fits are shown in Figure 9 [*b*]. It can be seen that the calculated values of E_∞^* strongly decay with an increase in the duration of creep time measured. Indeed, the plot of E_∞^* vs hold time suggests that the value of E_∞^* is asymptoting to a value at or very near zero. This is the result of the total measured creep increasing faster with time than the Kelvin model expects. One possible explanation is that it is not possible to extrapolate fits to predict creep at longer times because it is not possible to resolve extremely long time constants in the noisy shorter term data. Although any very long time constant creep rates must be present from the start of the creep period, the fitting process may assign these contributions in the fitted data to shorter time constants. Extrapolation of the fit will, therefore, reduce the creep rate prematurely. For other polymeric materials with time constants close to or less than the duration of creep measured, the model may yield a better prediction. Another possible explanation of the poor prediction of future creep in PS-3 by the Kelvin model is that there is a component of non-visco-elastic deformation/displacement being measured. It can be seen in Figure 4 that the three different creep experiments in PS-3 have different terminal creep rates ~~at the end~~ (from 10 to 14 pm/second); experiment #3 appears to be tending to a constant (non-zero) creep rate. Pure viscous flow, or visco-plastic deformation or thermal drift would maintain a creep rate that is constant with applied stress

(equivalent to an infinite time constant). Since uncorrected thermal or other displacement drift has already been discounted by direct measurement of the instrument drift and its environmental stability, and since plastic deformation would distort only the start of the fit, this leaves the remaining possibility, namely that purely viscous or visco-plastic deformation mechanisms may be present in the polymer.

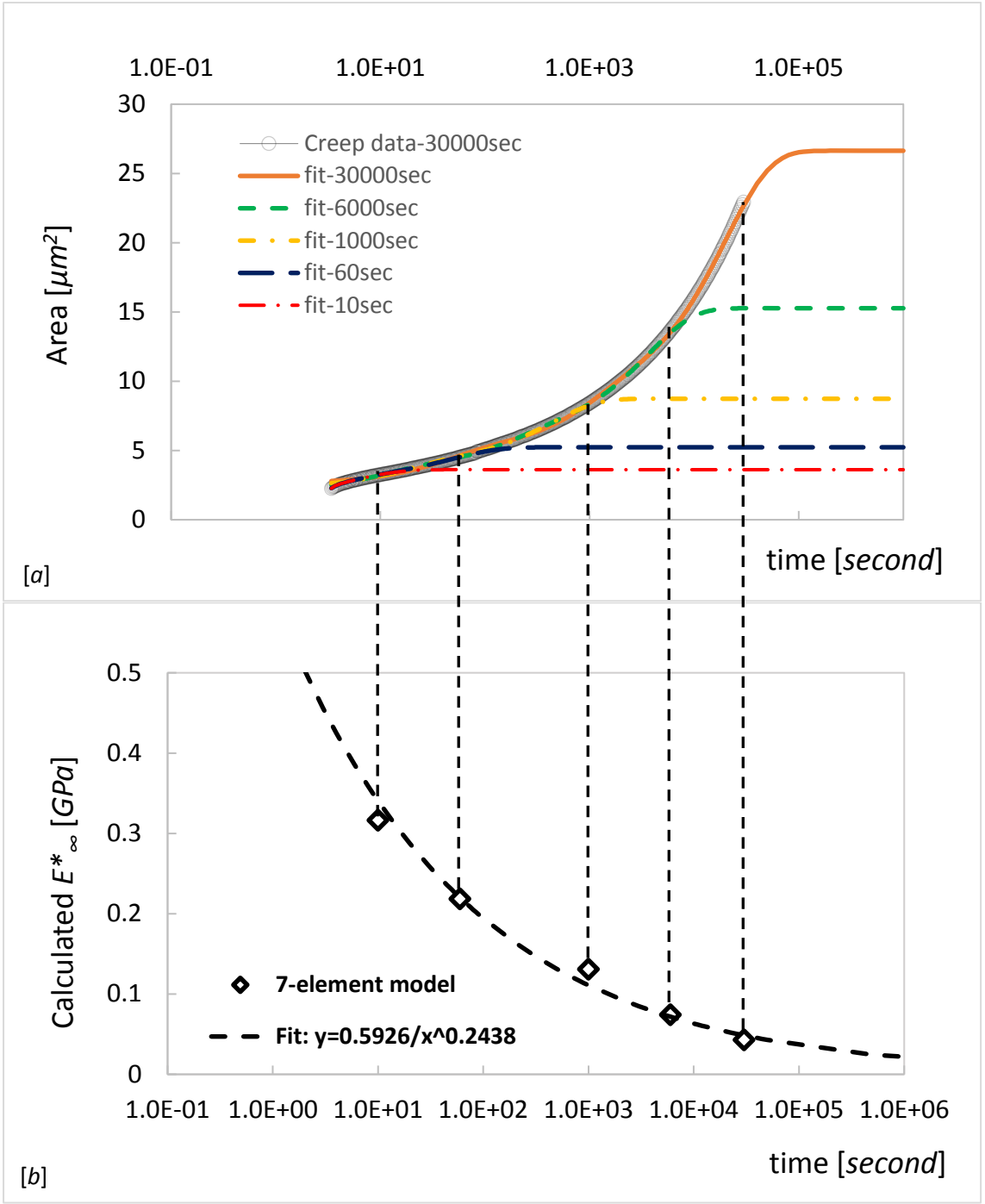

Figure 9 [*a*] indentation creep curve of PS-3 for 30000 seconds (experiment #3): plots of indentation area against creep time of experimental data, superposed the simulated curve calculated using the *N*-element Kelvin model (*N* =7, parameters obtained by fitting the 10, 60, 1000, 6000 and 30000 seconds); [*b*] a power law fit to the corresponding calculated infinite modulus $\boldsymbol{E}^*_\infty$ values.

The measurement of very long creep times shows up extremely clearly a problem that has not generally been discussed in the indentation creep literature (to our knowledge). This is the failure of the experiment to maintain a constant stress throughout the creep measurement. As the indenter creeps into the material under constant applied force, the indentation contact area increases and this reduces the applied stress of the indentation. In short duration indentation creep experiments, this may be less noticeable and has certainly, previously, been neglected. In the indentation data set plotted in Figure 4, the indentation depth at the beginning of the creep (t_0) is 682nm and even after only 10 seconds creep is 826 nm (21% increase in depth and a 42% increase in area). In the longest experiments here in Figure 6, the indentation depth increases from 682 nm at t_0 to over 2215 nm at 30000 seconds. This is over a factor of ten increase in area and, consequently, a factor of ten decrease in applied stress. Even if the material is purely visco-elastic, stress reduction results in a much reduced creep rate and, for much of the material in contact, a progressive creep recovery. It is clear that a proper simulation of long duration constant force creep experiments with large total creep displacements is only possible if both the creep compliance and the stress relaxation effects are considered. This is outside the scope of this paper. Our results show that, if the premises of the visco-elastic model are not to be broken and if constant force indentation creep measurements are to be used, there needs to be a limit set on the total amount of creep allowed, in addition to a limit on the minimum creep rate measurable. It might be expected that stiffer viscoelastic materials might not pose such a problem. However, if the total creep is expressed as a percentage of the initial indentation at maximum force, indentations in the fused silica and sapphire experiments exhibited an increased depth of 23% (18/77) and 4.2% (6/144) (approximately equivalent to an increase in contact area of 46% and 8.4%) for the fused silica and the sapphire respectively. Even if a 10% stress reduction could be tolerated, only the sapphire would qualify.

Based on the discussions above, the limits to indentation creep compliance measurement are, therefore, as follows:

1. Instrument sensitivity to environmental instability is unique to each instrument and its measurement will provide a minimum creep rate that can be measured validly. The particular properties of the material to be tested will result in this minimum creep rate occurring at a particular maximum creep time.
2. The analysis depends on the material tested to be elastic/viscoelastic and any pure plasticity or pure viscosity (or visco-plasticity) will distort the outputs of the analysis. Pure plasticity can be minimised by using low strain inducing indenter geometries.
3. The analysis requires the applied stress to be constant throughout the creep measurement. If the force is kept constant during the creep hold period, this places a maximum limit on the experimental measurement time, which will depend on the total amount of creep experienced. Alternatively the experiment should increment force to maintain a constant applied stress rather than a constant applied force.

5.3 A new method for prediction of E_∞^*

For long creep experiments, E_∞^* is an important parameter as it quantifies the total amount of creep accumulated in infinite time. This is useful for predicting the lifetime dimension change of polymeric material components. From the discussion in section 5.2, it's clear that the use of viscoelastic Kelvin model for calculating E_∞^* of PS-3 would yield poor predictions of future indentation creep, since the longer the creep, the smaller the calculated E_∞^* , as shown in Figure 9[*b*]. However, the trend itself can be used for better prediction of E_∞^* in the limit of infinite time. It is practically not possible to do an infinite time creep experiment, but a mathematical fit can be used to extrapolate the E_∞^* data points obtained at different creep time (10, 60, 1000, 6000, 30000 seconds) towards longer time. One candidate fitting function is suggested below:

Equation 1: $\boldsymbol{E_\infty^* = at^b}$ where *a* and *b* are fitting parameters.

The function is a reasonably good fit to the data points when *a* is 0.5926 and *b* is -0.2438 as shown in Figure 9[*b*]. Using this equation, E_{∞}^{*} of PS-3 is estimated to be 4 ± 1 MPa; the standard deviation was calculated based on the results from three repeated experiments. There are no literature values to do a comparison for such a long indentation creep study, but the authors are not surprised to have such a low value if PS-3 is visco-plastic since it would then be expected to creep continuously. This extrapolation method can be used to provide valuable information about infinite modulus at much longer creep times than are experimentally possible, or provide a measure of the visco-elastic nature of a material component – the more constant the value of E_{∞}^{*} the more predictably visco-elastic the material – or whether other deformation models might be more appropriate or longer time constants would be expected to exist in the viscoelastic material under investigation). If a viscoelastic material has limited number of time constants that are close to the duration of the creep measurement, the extrapolation is likely to predict E_{∞}^{*}) lower than the real value (as it assumes an infinite series of new and unmeasured time constants occurring at the same rate as observed in the measured data). This suggests this new method defines the lower boundary for infinite modulus, hence the maximum viscoelastic dimensional change under constant stress.

5. Conclusions

We have shown that the UNHT system provides extremely good stability when located in a well-controlled environment. The instrument reported here achieved a displacement drift < 0.2 pm/second, which enabled valid measurement of much lower creep rates over much longer indentation creep test durations (orders of magnitude longer) than has previously been possible. Valid, low-uncertainty, long-term creep data over test durations of 30000 seconds has been used to demonstrate the inability of a viscoelastic creep analysis model to obtain fit parameters from one duration of creep data and extrapolate those results to predict the creep behaviour at longer times.

Comparison of the goodness of fit of an *N*-element Kelvin model (3<*N*<15) to Indentation creep results for the material PS-3 show that the standard linear solid model (*N* = 3 elements) is inadequate to fit the creep response and more time constants are required, but that using more than *N*=7 elements (three time constants) does not improve the fit significantly.

We have shown that good fits to even extremely low uncertainty experimental data are not able to obtain all of the time-constants required to extrapolate the material response more than a short time into the future (approximately twice the creep test duration), and much less than the decade of time typically assumed in uniaxial rheological models.

We have proposed and demonstrated a new model to overcome the analysis limitations identified. This is a pragmatic attempt to predict the future behaviour of a material such as PS-3 from shorter duration test data and to provide results that are more independent of the creep test duration. We have shown that, where a valid measurement of indentation creep over several decades of time is possible, the variation in the value of E_{∞}^{*} (as a function of time-span of data fitted) may be used to predict more accurately the true E_{∞}^{*} value. In this case, we have shown that values of E_{∞}^{*} of ~0.2 GPa obtained by fits to 60 seconds of creep data extrapolate to an infinity value of only 4 MPa. The high quality of the data shows that this is not due to drift and so must be the consequence of a non-visco-elastic material response in PS-3.

The data presented here raises suspicions that the viscoelastic models available may be a poor model of actual indentation creep response. We provide a number of recommendations to improve indentation creep testing:

- Use of a large radius sphere, rather than a Berkovich indenter geometry, will reduce the pure plastic component, which may improve the viscoelastic model fit over short creep times. However, the rate of increase in area with depth is larger and this will reduce the creep rates measured for any particular force, which may restrict the materials and maximum length of creep test possible in a particular instrument.
- If a force controlled creep test is to be conducted, increment the applied force as a function of displacement in order to maintain a constant applied stress during the creep test. This will better match the experimental stress cycle to the one assumed in the creep analysis described here. Such algorithms could easily be made widely available as similar ones are already used to adjust for suspension spring stiffness in some instruments.

Further research is required to investigate whether a better approach may be to change the experiment to displacement control and the measurement of stress-relaxation. Instruments, such as the UNHT, that are able to measure force and conduct true displacement-controlled indentations are ideally placed to measure stress-relaxation instead of creep. However, a change of kinematic model to a general Maxwell model would be required to model stress-relaxation rather than creep. A new understanding of the effect of displacement drift on the measured force would also be required.

Acknowledgement

This project has received funding from the EMPIR programme co-financed by the Participating States and from the European Union's Horizon 2020 research and innovation programme: Grant Number 14IND03.The authors acknowledge collaboration with Anton Paar Ltd, who provided expertise and instrumentation for this work.

References

[1] R.Heuss, N.Muller, W.V. Sintern, A.Starke and A.Tschiesner, "Lightweight, heavy impact" (2012) Report of McKinsey&Compnay
[2] T. Brown, The Manufacturer (2014), http://www.themanufacturer.com/articles/high-performance-polymers-replacing-metals-demanding-applications/
[3] M.Y. Lyu and T.G. Choi, Int. J. Precis. Eng. Manuf. **16** (2015), p.213-220
[4] ISO 899-1:2003 Plastics — Determination of creep behaviour — Part 1: Tensile creep
[5] A.S. Maxwell, M.A. Monclus, N.M. Jennett and G. Dean, Polym. Test. **30** (2011), p.366-371
[6] P.S. Uskokovic, C.Y. Tang, C.P. Tsui, N. Ignjatovic and D.P. Uskokovic, J. Eur. Ceram. Soc. **27** (2007), p.1559-1564
[7] Y-T Chen, W.Ni and C-M Cheng, J. Mater. Res. **20** (2005), p.3061-3071
[8] M.L. Oyen and R.F. Cook, J. Mater. Res. **18** (2003), p.139-150
[9] NPL Report MATC(A)24 (2001) "Indicoat Final ReportDetermination of hardness and modulus of thin films and coatings by nanoindentation"
[10] ISO 14577-1:2015 Metallic materials - Instrumented indentation test of hardness and materials parameters Part 1: Test method
[11] V. Maier, B. Merle, M. Göken, K. Durst, J. Mater. Res. (2013) **28** p. 1177-1188
[12] J. Mencík, L.H. He, M.V. Swain, J. Mech. Behav. Biomed. Mater. **2** (2009) p.318-325
[13] C.A. Tweedie and K.J. Van Vliet, J Mater Res **21** (2006), p.1576–1589.
[14] M.A. Monclus and N.M. Jennett, Philos. Mag. **91** (2013), p. 1308-1328
[15] S. Yang, Y-W Zhang and K. Zeng, J.Appl.Phys. **95** (2004), p.3655-3666
[16] C.Y. Zhang, Y.W. Zhang, K.Y.Zheng and L.Shen, J. Mater. Res. **20** (2005), p. 1597-1605
[17] I.N. Sneddon, "Boussinesq's problem for a rigid cone", Proc. Cambridge Philos. Soc. (1948) **44** pp.492-507
[18] K.L. Johnson, Contact Mechanics, Cambridge University Press, Cambridge, 1985

[19] E.H. Lee and J.R.M. Radock, J. Appl. Mech. (1960) **27** p.438-444
[20] M.L. Oyen, J. Mater. Res. (2005) **20** p. 2094-2100
[21] M. V. Ramesh Kumar1 and R. Narasimhan, Current Science (2004) **87** p. 1088-1095
[22] J. Liu, C. Liu, J. Tan, B. Yang and T. Wilson, J. Microsc. (2016) **261** p. 300-306
[23] J. Nohava, N.X. Randall and N. Conte, J. Mater. Res. **24** (2009), p. 873-882
[24] http://www.vishaypg.com/docs/11222/11222BPhoto.pdf (accessed on 12 March 2018)
[25] M.L. Oyen, Acta Mater. (2007) **55** p.3633-3639
[26] European Project INDICOAT SMT-CT98-2249 Final Report Dertermination of Hardness and Modulus of Thin Films and Coatings by Nanoindentation, NPL report MATC(A) 24 (2011)

Appendix: additional viscoelastic analysis results

Table A1a. The creep dataset #1 obtained from PS-3 was truncated at different creep times: 10, 60, 1000, 6000 and 30000 seconds. The *N*-element Kelvin model (*N* = 7) was then used to fit each truncated dataset and the analysis results are summarised here, where E_0^* is the instant modulus, E_∞^* is the effective infinite modulus, τ_i is the time constants (*i* =1, 2 and 3) and E_i^* is the corresponding modulus for each of the time constant.

Creep time	E_∞^*	E_0^*	E_1^*	E_2^*	E_3^*	τ_1	τ_2	τ_3
[second]	[GPa]	[GPa]	[GPa]	[GPa]	[GPa]	[sec]	[sec]	[sec]
10	0.33	-8.71	0.80	1.59	0.78	0.31	1.80	15.99
60	0.26	3.30	0.85	1.59	0.56	0.65	4.73	50.44
1000	0.13	0.79	1.08	0.80	0.25	4.09	53.08	689.71
6000	0.07	0.60	0.78	0.43	0.12	18.21	299.70	5571.36
30000	0.06	0.54	0.56	0.31	0.10	44.75	891.14	12939.31

Table A1b. The creep dataset #2 obtained from PS-3 was truncated at different creep times: 10, 60, 1000, 6000 and 30000 seconds. The *N*-element Kelvin model (*N* = 7) was then used to fit each truncated dataset and the analysis results are summarised here, where E_0^* is the instant modulus, E_∞^* is the effective infinite modulus, τ_i is the time constants (*i* =1, 2 and 3) and E_i^* is the corresponding modulus for each of the time constant.

Creep time	E_∞^*	E_0^*	E_1^*	E_2^*	E_3^*	τ_1	τ_2	τ_3
[second]	[GPa]	[GPa]	[GPa]	[GPa]	[GPa]	[sec]	[sec]	[sec]
10	0.34	-91.15	0.90	1.67	0.80	0.35	1.46	11.20
60	0.26	3.68	0.82	1.44	0.58	0.63	4.56	47.38
1000	0.13	0.80	1.01	0.81	0.24	3.91	49.67	706.05
6000	0.09	0.49	∞	0.45	0.14	0.18	72.68	2567.70
30000	0.06	0.43	∞	0.29	0.09	0.02	226.26	9359.14

Table A1c. The creep dataset #3 obtained from PS-3 was truncated at different creep times: 10, 60, 1000, 6000 and 30000 seconds. The *N*-element Kelvin model (*N* = 7) was then used to fit each truncated dataset and the analysis results are summarised here, where E_0^* is the instant modulus, E_∞^* is the effective infinite modulus, τ_i is the time constants (*i* =1, 2 and 3) and E_i^* is the corresponding modulus for each of the time constant.

Creep time	E_∞^*	E_0^*	E_1^*	E_2^*	E_3^*	τ_1	τ_2	τ_3
[second]	[GPa]	[GPa]	[GPa]	[GPa]	[GPa]	[sec]	[sec]	[sec]
10	0.32	6.76	0.83	1.71	0.81	0.25	0.94	6.06
60	0.22	1.44	0.84	1.34	0.53	0.62	3.84	45.85
1000	0.12	0.60	0.93	0.69	0.23	3.61	55.83	786.65
6000	0.07	0.51	0.79	0.45	0.12	9.36	180.24	3832.71
30000	0.04	0.42	0.55	0.28	0.07	40.16	849.08	18543.16

Table A2a. Analysis results obtained by fitting to 30000 seconds experimental creep curve of PS-3 dataset #1, using the generalised *n*-time-constant (*N = 2n+1* elements) Kelvin model (time constants *n* = 1, 2, 3, 4, 5, 6, 7 and number of elements *N* = 3, 5, 7, 9, 11, 13, 15), where τ_i is the calculated time constant (*i* = 1, 2, 3, 4, 5, 6, 7) and E_i^* is the corresponding modulus for each time constant.

Number of elements	τ_1	τ_2	τ_3	τ_4	τ_5	τ_6	τ_7
-	[sec]	[sec]	[sec]	[sec]	[sec]	[sec]	[sec]
3	4178.81	-	-	-	-	-	-
5	210.45	8910.35	-	-	-	-	-
7	44.75	891.14	12939.31	-	-	-	-
9	11.82	185.15	2138.17	19047.41	-	-	-
11	0.05	11.82	185.17	2138.39	19048.75	-	-
13	0.05	0.05	11.82	185.15	2138.18	19047.51	-
15	0	0.05	0.05	11.82	185.15	2138.18	19047.52

Number of elements	E_1^*	E_2^*	E_3^*	E_4^*	E_5^*	E_6^*	E_7^*
-	[GPa]	[GPa]	[GPa]	[GPa]	[GPa]	[GPa]	[GPa]
1	0.09	-	-	-	-	-	-
3	0.30	0.09	-	-	-	-	-
5	0.56	0.31	0.10	-	-	-	-
7	0.89	0.50	0.28	0.10	-	-	-
9	∞	0.89	0.50	0.28	0.10	-	-
11	∞	∞	0.89	0.50	0.28	0.10	-
13	∞	∞	∞	0.89	0.50	0.28	0.10

Table A2b. Analysis results obtained by fitting to 30000 seconds experimental creep curve of PS-3 dataset #2, using the generalised *n*-time-constant (*N = 2n+1* elements) Kelvin model (time constants *n* = 1, 2, 3, 4, 5, 6, 7 and number of elements *N* = 3, 5, 7, 9, 11, 13, 15), where τ_i is the calculated time constant (*i* = 1, 2, 3, 4, 5, 6, 7) and E_i^* is the corresponding modulus for each time constant.

Number of elements	τ_1	τ_2	τ_3	τ_4	τ_5	τ_6	τ_7
-	[sec]	[sec]	[sec]	[sec]	[sec]	[sec]	[sec]
3	4307.04	-	-	-	-	-	-
5	226.26	9359.19	-	-	-	-	-
7	0.02	226.26	9359.14	-	-	-	-
9	0	0.02	226.24	9358.9	-	-	-
11	0	0	0.02	226.2	9358.86	-	-
13	0	0	0	0.02	226.24	9358.86	-
15	0	0	0	0	0.02	226.24	9358.89

Number of elements	E_1^*	E_2^*	E_3^*	E_4^*	E_5^*	E_6^*	E_7^*
-	[GPa]	[GPa]	[GPa]	[GPa]	[GPa]	[GPa]	[GPa]
1	0.09	-	-	-	-	-	-
3	0.29	0.09	-	-	-	-	-
5	∞	0.29	0.09	-	-	-	-
7	∞	∞	0.29	0.09	-	-	-
9	∞	∞	∞	0.29	0.09	-	-
11	∞	∞	∞	∞	0.29	0.09	-
13	∞	∞	∞	∞	∞	0.29	0.09

Table A2c. Analysis results obtained by fitting to 30000 seconds experimental creep curve of PS-3 dataset #3, using the generalised *n*-time-constant (*N = 2n+1* elements) Kelvin model (time constants *n* = 1, 2, 3, 4, 5, 6, 7 and number of elements *N* = 3, 5, 7, 9, 11, 13, 15), where τ_i is the calculated time constant (*i* = 1, 2, 3, 4, 5, 6, 7) and E_i^* is the corresponding modulus for each time constant.

Number of elements	τ_1	τ_2	τ_3	τ_4	τ_5	τ_6	τ_7
-	[sec]	[sec]	[sec]	[sec]	[sec]	[sec]	[sec]
3	5552.48	-	-	-	-	-	-
5	149.81	11353.51	-	-	-	-	-
7	40.16	849.08	18543.16	-	-	-	-
9	0.01	40.17	849.22	18544.40	-	-	-
11	0.01	0.01	40.17	849.24	18544.55	-	-
13	0.01	0.01	6.84	121.72	1533.60	23884.42	-
15	0	0.01	0.01	6.84	121.72	1533.61	23884.52

Number of elements	E_1^*	E_2^*	E_3^*	E_4^*	E_5^*	E_6^*	E_7^*
-	[GPa]	[GPa]	[GPa]	[GPa]	[GPa]	[GPa]	[GPa]
1	0.07	-	-	-	-	-	-
3	0.29	0.07	-	-	-	-	-
5	0.55	0.28	0.07	-	-	-	-
7	∞	0.55	0.28	0.07	-	-	-
9	∞	∞	0.55	0.28	0.07	-	-
11	∞	∞	0.86	0.51	0.29	0.06	-
13	∞	∞	∞	0.86	0.51	0.29	0.06